

Room temperature luminescence of passivated InGaN quantum dots formed by quantum-sized-controlled photoelectrochemical etching

Xiongliang Wei, Syed Ahmed Al Muyeed, Matthew R. Peart, Wei Sun, Nelson Tansu, and Jonathan J. Wierer

Citation: *Appl. Phys. Lett.* **113**, 121106 (2018); doi: 10.1063/1.5046857

View online: <https://doi.org/10.1063/1.5046857>

View Table of Contents: <http://aip.scitation.org/toc/apl/113/12>

Published by the [American Institute of Physics](#)

AIP | Conference Proceedings

Get **30% off** all
print proceedings!

Enter Promotion Code **PDF30** at checkout



Room temperature luminescence of passivated InGaN quantum dots formed by quantum-sized-controlled photoelectrochemical etching

Xiongliang Wei,^{a)} Syed Ahmed Al Muyeed, Matthew R. Peart, Wei Sun, Nelson Tansu,^{b)} and Jonathan J. Wierer, Jr.^{c)}

Center for Photonics and Nanoelectronics, Department of Electrical and Computer Engineering, Lehigh University, Bethlehem, Pennsylvania 18015, USA

(Received 2 July 2018; accepted 2 September 2018; published online 18 September 2018)

Room temperature luminescence of epitaxial InGaN quantum dots (QDs) formed by quantum sized-controlled photoelectrochemical (QSC-PEC) etching and passivation layer regrowth is demonstrated. QSC-PEC etching is performed on a 7.5 nm thick $\text{In}_{0.20}\text{Ga}_{0.80}\text{N}$ layer emitting at $\sim 514\text{--}521$ nm and with a laser diode emitting at 445 nm. Parameters such as etch bias (0.9 V and 1.5 V), laser average power (20 mW/cm² and 100 mW/cm²), and laser operating conditions (pulsed and continuous wave) are explored. QSC-PEC etching of $\text{In}_{0.20}\text{Ga}_{0.80}\text{N}$ requires a minimum bias (>0.9 V) and pulsed laser conditions in order to form QDs. After etching, the QDs do not exhibit photoluminescence due to defect recombination. Regrowth of passivation layers consisting of a 2 nm thick $\text{Al}_{0.45}\text{Ga}_{0.55}\text{N}$ layer and a 11 nm thick GaN layer reduce the defect recombination, and room temperature photoluminescence is observed at room temperature at $\sim 435\text{--}445$ nm with narrow full-width at half-maximum of ~ 35 nm. Published by AIP Publishing. <https://doi.org/10.1063/1.5046857>

III-nitride emitters can be very efficient and InGaN-based light-emitting diodes (LEDs) for solid-state lighting (SSL) are notable because they are the most efficient sources of light ever created.^{1,2} However, high-efficiency InGaN-based LEDs can only be achieved at low current densities ($>80\%$, ~ 5 A/cm²)² and thresholds of InGaN-based laser diodes (LDs) also limit peak efficiency.^{3,4} Both emitters use quantum wells (QWs) as the active light-emitting material that are limited in radiative efficiency because parasitic indirect Auger recombination. Auger recombination is a fundamental problem in III-nitrides as demonstrated experimentally^{5–7} and causes the decrease in efficiency at high current densities (“efficiency droop”) in LEDs.

The use of epitaxial InGaN quantum dot (QD) as the light-emitting active layers may be a method to suppress Auger recombination⁸ and solve the “efficiency droop” in III-nitride LEDs.³ Indeed, lower Auger recombination rates have been observed in colloidal QDs as the size is reduced.⁹ InGaN-based QD emitters can have higher differential gain and higher spontaneous emission rates compared to conventional InGaN QWs, and this can translate to lower threshold currents for LDs and higher efficiencies at higher current densities for LEDs. These benefits are well-known from previous work¹⁰ and can only be realized if the inhomogeneous broadening can be controlled. This requires a synthesis method that can control the size or quantum states of the QD ensembles. If this can be achieved, then InGaN-based QD emitters have a great opportunity to produce higher efficiency light emitters for application such as SSL or displays.

Much effort has been put into research of QD active layers in various semiconductor material systems.^{11–14} For epitaxial QDs, the most common and successful method is

Stranski-Krastanov (SK) growth.¹⁵ In this method, strain between the QD layer and the underlying layers leads to 3-dimensional growth and the formation of QDs. QDs formed in this method have resulted in extremely low threshold currents in InAs QD LDs.¹⁶ SK growth can also be used to synthesize InGaN QDs, but there is a lack of dimensional control, and also low dot densities ($<100/\mu\text{m}^2$),^{17–22} that limits their efficiency performance below that of QWs. An alternative approach is to use diblock copolymer lithography and selective-area epitaxy to form InGaN QDs at achieve higher dimensional control,²³ but this approach is still limited to larger size dots.

Recently, a new method called quantum-sized-controlled photoelectrochemical (QSC-PEC) etching²⁴ has been developed to overcome the size and density limitations of Stranski-Krastanov growth. The critical difference from traditional GaN-based photoelectrochemical etching²⁵ is the use of a coherent laser source. QSC-PEC etching proceeds by absorption of the laser light only in the InGaN layer, and the additional electrolyte and bias causes etching via oxidation of InGaN and dissolution of this oxide layer.²⁶ Eventually the etch self-terminates because the InGaN forms into QDs that are small enough that they can no longer absorb the laser light. Theoretically by changing the exciting wavelength and indium composition in the InGaN layers, one can control the quantum size of the QDs very precisely and with relatively high QD densities (up to $1100/\mu\text{m}^2$).²⁴ Violet-emitting QDs have been synthesized using the QSC-PEC process beginning with blue-emitting InGaN thin films.²⁴ However, the photoluminescence (PL) of QSC-PEC etched QDs has only been demonstrated at cryogenic temperatures (5 K)²⁴ most likely due to the high defect and surface recombination present on the exposed QD surfaces.

In this letter, room temperature photoluminescence (PL) from InGaN QDs emitting in the blue and formed by QSC-PEC is demonstrated. The QDs are formed from $\text{In}_{0.20}\text{Ga}_{0.80}\text{N}$

^{a)}Email: xiw314@lehigh.edu

^{b)}Email: Tansu@lehigh.edu

^{c)}Email: jwierer@lehigh.edu

thin films that emit at $\sim 514\text{--}521$ nm across the wafer, and the QSC-PEC process uses a blue (445 nm) LD as the coherent light source. Different etching strategies are presented including varying the etch bias and peak power of the laser. As-etched (exposed) QDs do not exhibit PL, so passivation layers consisting of $\text{Al}_{0.45}\text{Ga}_{0.55}\text{N}/\text{GaN}$ are grown on the QD samples to recover the PL. These passivated QDs exhibit room temperature PL whose peak wavelength varies from 435 to 445 nm depending on temperature or size of the QDs.

The QDs are formed using the QSC-PEC etch process using the apparatus shown in Fig. 1(a). The conditions are similar to previous reports^{24,26} using a 0.2 M H_2SO_4 electrolyte, a Ag/AgCl reference electrode, a Pt counter electrode, a potentiostat to bias and measure the current, and a 445 nm laser diode with a linewidth of ~ 4 nm. The laser source is directed through a diffractive element to expose a large portion of the InGaN sample. The samples are grown in a vertical-type metalorganic chemical vapor deposition (MOCVD) reactor by depositing 7.5 nm ($\pm 5\%$) thick $\text{In}_{0.20}\text{Ga}_{0.80}\text{N}$ layers [Fig. 1(b)] on 2-inch diameter, n-type GaN templates at a temperature of 730°C and a growth pressure of 200 torr. PL is measured using an argon ion laser with powers of ~ 55 mW (diameter ~ 500 μm) at 351 nm, and the emitted light is collected into a fiber that is directed to a spectrometer to measure the spectra. The $\text{In}_{0.20}\text{Ga}_{0.80}\text{N}$ layer has a peak in emission at $\sim 514\text{--}521$ nm, with an indium variation $< 1\%$, and PL intensity variation of $\sim 10\%$ across the wafer at the low power densities used in this study. The wafers are cut into smaller rectangular pieces (0.5 cm \times 1.5 cm) to test the etch parameters, and “1/6” pie-shaped pieces for QD etching and passivation layer growth via MOCVD. The etch bias is either 0.9 V or 1.5 V and the average power density is 20 mW/cm² or 100 mW/cm² in both continuous wave or pulsed mode (5% duty cycle, at 20 kHz). Etch times are between 20 and 30 min resulting in QDs as shown schematically in Fig. 1(c). The pie-shaped samples are cleaned by sonicating in isopropyl alcohol for 15 min, dried with ionized nitrogen, and then subject to passivation layer growth consisting of a 2 nm thick $\text{Al}_{0.45}\text{Ga}_{0.55}\text{N}$ layer followed by a 11 nm thick undoped GaN layer as shown

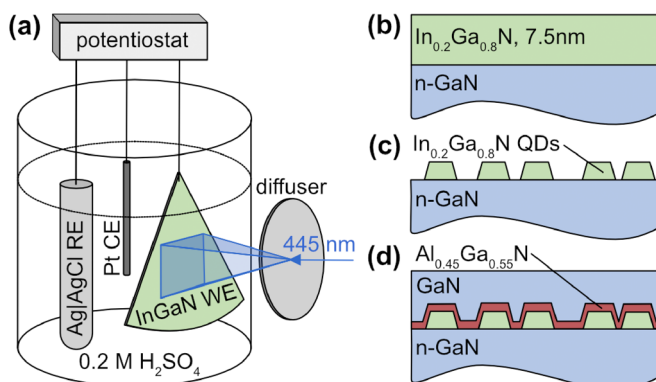


FIG. 1. Schematic of (a) the quantum-size-controlled photoelectrochemical etch apparatus using a 445 nm laser diode, a Ag/AgCl reference electrode (RE), a Pt counter electrode (CE), and 0.2 M H_2SO_4 electrolyte. Cross-sectional schematic of the (b) as-grown, 7.5 nm thick $\text{In}_{0.2}\text{Ga}_{0.8}\text{N}$ layer on an n-type GaN/sapphire template, (c) $\text{In}_{0.2}\text{Ga}_{0.8}\text{N}$ quantum dots (QDs) formed after etching, and (d) $\text{In}_{0.2}\text{Ga}_{0.8}\text{N}$ QDs after growth of a passivation layer consisting of 2 nm thick $\text{Al}_{0.4}\text{Ga}_{0.6}\text{N}$ and 2 nm thick GaN layer.

in Fig. 1(d). An atomic force microscope (AFM) is used to image the QDs after etching and passivation layer growth.

To illustrate how the etch conditions can affect the formation of the InGaN QDs, Fig. 2 shows AFM images of an unetched InGaN layer and QD layers after PEC etching under various conditions. The unetched sample [Fig. 2(a)] shows a “brain-like” morphology of the 7.5 nm thick $\text{In}_{0.2}\text{Ga}_{0.8}\text{N}$ films with flat areas separated by deeper trenches that bend throughout the structure. These films are then QSC-PEC etched with three different etch conditions and at the same etch time of 20 min. Figure 2(b) shows the InGaN sample etched with a continuous wave laser power of 20 mW/cm² at a bias of 0.9 V. Here, the light intensity and bias conditions are not high enough to create a positive InGaN/electrolyte interface and promote oxidation and etching. There is only a slight change in the sample compared to the unetched sample and it is consistent with a low etch current. Some slight etching is observed with a rougher surface and slightly wider trenches.

In order to promote etching and QD formation, higher light intensities and bias conditions are necessary. Figure 2(c) shows the sample etched under similar condition as Fig. 2(b) except the bias is increased to 1.5 V. The sample shows nanostructure formation, but it cannot be classified as QDs because the islands are too large and are not separated in some cases. Under this higher bias, the InGaN energy band at the InGaN/electrolyte interface are bent further up due to the larger bias, and this creates a hole concentration at the interface that promotes oxidation and etching of the InGaN surface. Calculations of the Fermi-level (E_F) position for an unbiased InGaN layer, assuming an electron concentration of $10^{17}/\text{cm}^3$, show that E_F is ~ 1 V above the intrinsic energy level, and therefore the bias conditions in Fig. 2(b) are too low to produce and contain the holes created by light

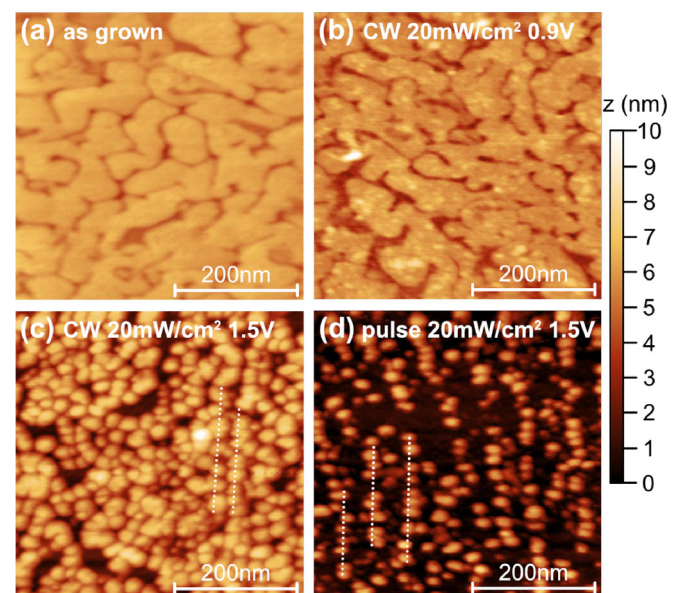


FIG. 2. Atomic force microscope (AFM) images of (a) an unetched InGaN sample, (b) an InGaN sample etched with a continuous wave power of 20 mW/cm² and a bias of 0.9 V, (c) an InGaN sample etched with a continuous wave power of 20 mW/cm² and a bias of 1.5 V, and (d) an InGaN sample etched with an average pulsed power of 20 mW/cm² (5% duty cycle, 20 kHz) and a bias of 1.5 V. All samples are etched for 20 min. The higher bias and laser peak power leads to QD formation. The dotted lines highlight QDs aligned to atomic steps.

absorption at the surface. It is interesting that the islands are in alignment with the underlying atomic steps of the GaN, which is based on AFMs of the GaN templates (not shown). The InGaN film at these steps is not flat and should affect the etching rate. It is possible that the InGaN layer experience differences in polarization induced fields and a resulting difference in bias at these locations that slightly inhibits and seeds QD formation. Indeed, the QDs seem to form on or close to these atomic steps indicating a reduced etch bias.

Figure 2(d) shows the sample etched under the same condition as Fig. 2(c) except with pulsed laser conditions at 20 kHz, 5% duty cycle, and average power of 20 mW/cm². The QD density is $\sim 800/\mu\text{m}^2$, and the small islands are separated further and shrink to even smaller size to form QDs. The QDs have a diameter that is ~ 20 nm and height that is ~ 5 nm. (Note the AFM is artificially stretching the QDs in the horizontal direction due to the tip and scan speed, and the diameter is taken in the vertical direction.) The pulsed laser light is producing higher peak power, and this creates a larger number of positive charge at the InGaN/electrolyte interface possibly due to nonlinear absorption for more efficient etching. Alternatively, the pulsing could allow for oxidation and reduction to proceed more efficiently where the InGaN film oxidizes during the pulse and reduces in the off state. It should be noted that the size distribution of the QDs shown here is larger than previous reports using a Ti-sapphire laser for etching,²⁴ which can be attributed to the larger linewidth of the laser diode, the broader emission from the initial film, variations in the film composition and thickness, surface roughness and morphology of the initial film, and stability of the laser exposure set up. However, similar to previous reports, the etch current is high at the beginning of the etch and decreases as the light absorption changes during etching.

Figure 3 shows AFM images of QDs with and without Al_{0.45}Ga_{0.55}N/GaN passivation layers at two different locations on the pie-shaped sample etched for ~ 30 min. The conditions are similar to the sample shown in Fig. 2(d) except the average laser pulse power is 100 mW/cm² to further shrink the QD size. The QDs in Fig. 3(a) are located at the approximate middle of the sample and etched with direct laser light, and the QDs in Fig. 3(b) are on an edge of the sample and occur just incident scattering light (unknown intensity) during etching. The QDs in the middle of the sample [Fig. 3(b)] have smaller size and a smaller dot density compared to the QDs formed from indirect light with approximate diameters of 20 nm and heights of 5 nm. This allows for comparison of different QD sizes and densities on the same sample. At these pump power densities, the QDs do not produce photoluminescence due to high defect recombination (e. g. point defects and surfaces).

These QDs are then subject to regrowth of passivation layers consisting of the 2 nm thick Al_{0.45}Ga_{0.55}N and 11 nm thick GaN. The AlGaIn layer is grown at 720 °C and the temperature is then raised to 905 °C to grow the GaN. This sequence is similar to multiple quantum well structures with AlGaIn interlayers used for LEDs emitting in the green-red.^{27–29} The low temperature AlGaIn layer is intended to cap the InGaIn and prevent decomposition and loss of indium during regrowth. Bare QDs exposed to an anneal in N₂ for

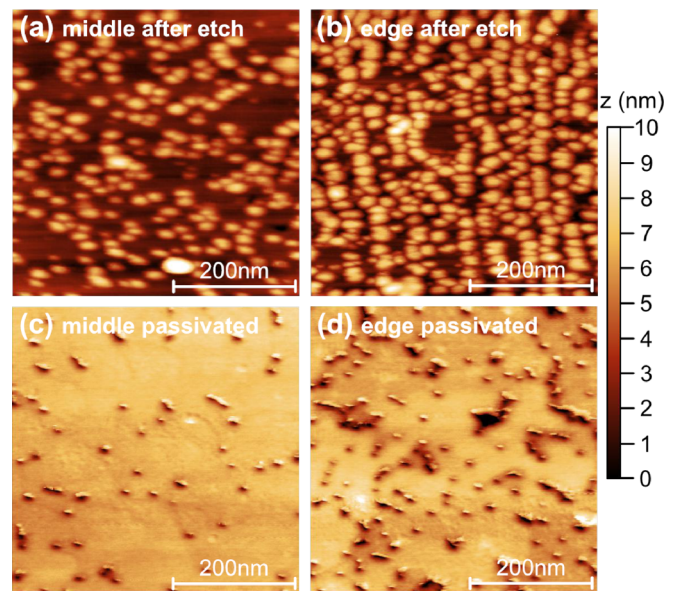


FIG. 3. AFM images of (a) QDs in the middle of the sample with direct laser emission at 100 mW/cm², and (b) QDs at the edge of the sample with indirect (scattering) light. Both are etched at a bias of 1.5 V and for ~ 30 min. The QDs in the middle of the sample are smaller in size and have a higher density. AFM images at the middle (c) and edge (d) of the sample after regrowth of the AlGaIn/GaN passivation layers. Most of the surface is extremely flat with some pitting that scales with the QD dot density.

2 min at the same temperature show no appreciable change in size, shape, and density. After AlGaIn capping, the GaN layer is grown which further passivates the InGaIn QDs and protects from reorganization, and the higher growth temperature anneal and promotes reduction of defects in the InGaIn layer. These positive effects have been observed in InGaIn QWs with high In content employing the AlGaIn/GaN growth and temperature sequence.²⁸ Growth of GaN passivation layers at various temperatures are not as effective as this passivation scheme (data not shown). Figures 3(c) and 3(d) show AFM images after regrowth of the passivation layers. The topography of regrown sample surface is mostly flat with a variation of less than 0.5 nm. However, there is some pitting on the surface and the density of pits scales with the density of QDs, suggesting the pits are due to the QDs. Also, it is possible that the QD shape could change slightly during regrowth and this is not revealed in these AFMs. Further work is necessary to understand any QD shape changes and eliminate these pits.

The growth of the passivation layers recovers the luminescence of the QDs. Figures 4(a) and 4(b) show the PL from the two different areas (Fig. 3) and at different temperatures. The QDs in the middle exhibit a PL peak at ~ 435 nm and at 77 K, and this PL peak red shifts to ~ 439 nm at 300 K. The PL intensity is low, and the “yellow band” emission from the GaN³⁰ is visible in the plot at longer wavelengths. For the edge of the sample with a higher QD density the PL peak is at ~ 439 nm at 77 K, and the peak red shifts to 443 nm at 300 K. The higher QD density leads to higher intensity, and the yellow band is less visible. It should be noted that the QDs shown here exhibit a narrow full-width at half-maximum (FWHM) at 35 nm which is at the low range of QD formed by SK growth^{17–20} due to the high dimensional control.

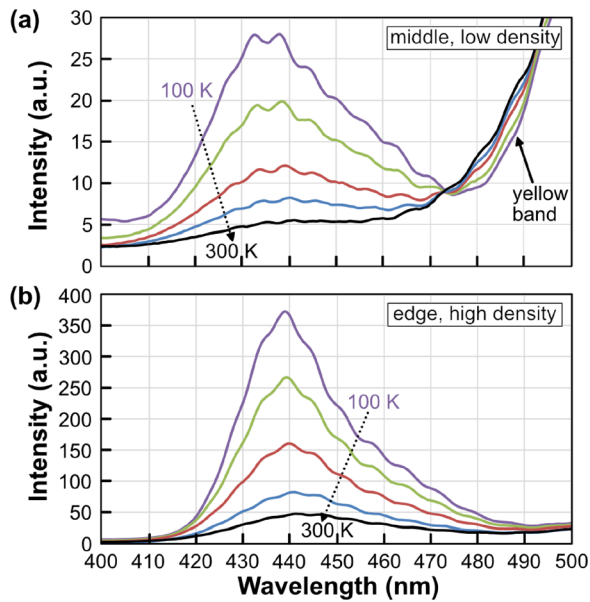


FIG. 4. Plots of photoluminescence intensity versus wavelength and temperature of the passivated QDs at the (a) middle area with lower QD density as shown in Figs. 3(a) and 3(c), and (b) at the edge with higher QD density shown in Figs. 3(b) and 3(d). Both plots are on the same intensity scale and the higher density QDs have ~ 10 times higher intensity. The emission of the edge QDs are slightly blue shifted from the middle QDs.

In conclusion, InGaN QDs formed by QSC-PEC etching and regrowth of AlGaIn/GaN passivation layers is demonstrated. To form the QDs, a minimum bias and pulsed laser light is required. These results also confirm the importance of passivation layer growth in etch-based epitaxial QDs in order to reduce defect recombination that prohibits luminescence. This demonstration shifted the PL from the green (QW) to the blue (QDs) which could be interesting for displays or SSL. The passivated QDs exhibit room temperature photoluminescence at $\sim 435\text{--}445$ nm, narrow FWHM ~ 35 nm, and the intensity of the QDs is higher with a higher QD density.

The authors would like to acknowledge funding from U.S. National Science Foundation (Awards No. 1408051, 1505122, and 1708227), and the Daniel E. '39 and Patricia M. Smith Endowed Chair Professorship Fund (N.T.).

¹J. Y. Tsao, M. H. Crawford, M. E. Coltrin, A. J. Fischer, D. D. Koleske, G. S. Subramania, G. T. Wang, J. J. Wierer, and R. F. Karliceck, *Adv. Opt. Mater.* **2**, 809 (2014).

²C. A. Humi, A. David, M. J. Cich, R. I. Aldaz, B. Ellis, K. Huang, A. Tyagi, R. A. DeLille, M. D. Craven, F. M. Steranka, and M. R. Krames, *Appl. Phys. Lett.* **106**, 031101 (2015).

- ³J. J. Wierer, N. Tansu, A. J. Fischer, and J. Y. Tsao, *Laser Photonics Rev.* **10**, 612 (2016).
- ⁴J. J. Wierer and J. Y. Tsao, *Phys. Status Solidi* **212**, 980 (2015).
- ⁵Y. C. Shen, G. O. Mueller, S. Watanabe, N. F. Gardner, A. Munkholm, and M. R. Krames, *Appl. Phys. Lett.* **91**, 141101 (2007).
- ⁶A. Laubsch, W. Bergbauer, M. Sabathil, M. Strassburg, H. Lugauer, M. Peter, T. Meyer, G. Brüderl, J. Wagner, N. Linder, K. Streubel, and B. Hahn, *Phys. Status Solidi* **6**, S885 (2009).
- ⁷J. Iveland, L. Martinelli, J. Peretti, J. S. Speck, and C. Weisbuch, *Phys. Rev. Lett.* **110**, 177406 (2013).
- ⁸J. L. Pan, *Phys. Rev. B* **46**, 3977 (1992).
- ⁹I. Robel, R. Gresback, U. Kortshagen, R. D. Schaller, and V. I. Klimov, *Phys. Rev. Lett.* **102**, 177404 (2009).
- ¹⁰D. Bimberg, M. Grundmann, and N. N. Ledentsov, *Quantum Dot Heterostructures* (John Wiley, 1999).
- ¹¹M. V. Maximov, A. F. Tsatsul'nikov, B. V. Volovik, D. A. Bedarev, A. Y. Egorov, A. E. Zhukov, A. R. Kovsh, N. A. Bert, V. M. Ustinov, P. S. Kop'ev, Z. I. Alferov, N. N. Ledentsov, D. Bimberg, I. P. Soshnikov, and P. Werner, *Appl. Phys. Lett.* **75**, 2347 (1999).
- ¹²T. Miyazawa, K. Takemoto, Y. Sakuma, S. Hirose, T. Usuki, N. Yokoyama, M. Takatsu, and Y. Arakawa, *Jpn. J. Appl. Phys.* **44**, L620 (2005).
- ¹³B. Daudin, F. Widmann, G. Feuillet, Y. Samson, M. Arlery, and J. L. Rouvière, *Phys. Rev. B* **56**, R7069 (1997).
- ¹⁴N.-M. Park, C.-J. Choi, T.-Y. Seong, and S.-J. Park, *Phys. Rev. Lett.* **86**, 1355 (2001).
- ¹⁵I. N. Stranski and L. Von Krastanow, *Abh. Math.-Naturwiss. Kl. III. Akad. Wiss. Wien* **146**, 797 (1938).
- ¹⁶D. Bimberg and N. Ledentsov, *J. Phys.: Condens. Matter* **15**, R1063 (2003).
- ¹⁷K. Tachibana, T. Someya, and Y. Arakawa, *Appl. Phys. Lett.* **74**, 383 (1999).
- ¹⁸C. Adelman, J. Simon, G. Feuillet, N. T. Pelekanos, B. Daudin, and G. Fishman, *Appl. Phys. Lett.* **76**, 1570 (2000).
- ¹⁹Y.-L. Chang, J. L. Wang, F. Li, and Z. Mi, *Appl. Phys. Lett.* **96**, 013106 (2010).
- ²⁰K. Tachibana, T. Someya, S. Ishida, and Y. Arakawa, *Appl. Phys. Lett.* **76**, 3212 (2000).
- ²¹Y.-K. Ee, H. Zhao, R. A. Arif, M. Jamil, and N. Tansu, *J. Cryst. Growth* **310**, 2320 (2008).
- ²²A. Kadir, C. Meissner, T. Schwaner, M. Pristovsek, and M. Kneissl, *J. Cryst. Growth* **334**, 40 (2011).
- ²³G. Liu, H. Zhao, J. Zhang, J. Park, L. J. Mawst, and N. Tansu, *Nanoscale Res. Lett.* **6**, 342 (2011).
- ²⁴X. Xiao, A. J. Fischer, G. T. Wang, P. Lu, D. D. Koleske, M. E. Coltrin, J. B. Wright, S. Liu, I. Brener, G. S. Subramania, and J. Y. Tsao, *Nano Lett.* **14**, 5616 (2014).
- ²⁵C. Youtsey, G. Bulman, and I. Adesida, *J. Electron. Mater.* **27**, 282 (1998).
- ²⁶X. Xiao, P. Lu, A. J. Fischer, M. E. Coltrin, G. T. Wang, D. D. Koleske, and J. Y. Tsao, *J. Phys. Chem. C* **119**, 28194 (2015).
- ²⁷J. Il Hwang, R. Hashimoto, S. Saito, and S. Nunoue, *Appl. Phys. Express* **7**, 071003 (2014).
- ²⁸D. D. Koleske, A. J. Fischer, B. N. Bryant, P. G. Kotula, and J. J. Wierer, *J. Cryst. Growth* **415**, 57 (2015).
- ²⁹S. A. Al Mueyed, W. Sun, X. Wei, R. Song, D. D. Koleske, N. Tansu, and J. J. Wierer, *AIP Adv.* **7**, 105312 (2017).
- ³⁰M. Julkarnain, N. Kamata, T. Fukuda, and Y. Arakawa, *Opt. Mater.* **60**, 481 (2016).